VEHICLE SYSTEM DYNAMICS
https://doi.org/10.1080/00423114.2025.2520492

OPEN ACCESS Check for updates

Toward intuitive drift assist control: driver drift intention recognition using a data-based approach

Yiwen Sun[a], Efstathios Velenis[a] and Ajinkya Krishnakumar[b]

[a]Advanced Vehicle Engineering Centre, Cranfield University, Bedford, UK; [b]Rimac Technology, Zagreb, Croatia

ABSTRACT

In contrast to autonomous drifting where path-planning determines when and where the vehicle drifts, to support drift-assist control systems in the framework of Advanced Driving Assistance System (ADAS), the human driver's intention needs to be recognised before the system intervenes with its assist functionality to facilitate drifting at the desired moment. We propose a method based on Bidirectional Long Short-Term Memory Network (Bi-LSTM) to interpret driver's intention to start/exit drifting, utilising only basic driver inputs and vehicle state signals. Firstly, to comprehensively understand driver's behaviour during drifting, we discuss the distinctive features in throttle and steering inputs and the corresponding vehicle acceleration signals during drift cornering and normal cornering, respectively. Next, two Bi-LSTM models are designed separately for the recognition of the 'Intention to Start Drifting' and the 'Intention to Exit Drifting'. Then, these models are trained and evaluated through a data set that contains over 500 laps of driving collected from the racing simulator Assetto Corsa. To validate the proposed approach, test sets of different drivers, track layouts and car models are adopted. The proposed intention recognition models successfully reach an accuracy of over 90% in recognising the two concerned intentions and outperform other classification methods in comparison.

ARTICLE HISTORY
Received 13 December 2024
Revised 2 June 2025
Accepted 10 June 2025

KEYWORDS
Drift-assist control; driver intention recognition; advanced driver assist system (ADAS); vehicle dynamics

Introduction

The technique of drifting is characterised by high sideslip angles and counter steering combined with throttle modulation during vehicle cornering, where the direction of the yaw rate opposes the steering input [1]. Associated with extreme manoeuvres, racing performance and active safety system designs [2,3], drifting generally demands a high level of driving proficiency from experienced drivers or the support of an intricate control system [4,5] to carefully balance throttle and steering inputs, in order to sustain an unstable equilibrium in vehicle dynamics [6,7].

Recently, a substantial amount of research has concentrated on autonomous drifting, where it is crucial to have an understanding of the desired trajectory and vehicle behaviour beforehand. Specifically, considering known track geometry (circular track [8–11] and

CONTACT Efstathios Velenis e.velenis@cranfield.ac.uk

© 2025 The Author(s). Published by Informa UK Limited, trading as Taylor & Francis Group.
This is an Open Access article distributed under the terms of the Creative Commons Attribution License (http://creativecommons.org/licenses/by/4.0/), which permits unrestricted use, distribution, and reproduction in any medium, provided the original work is properly cited. The terms on which this article has been published allow the posting of the Accepted Manuscript in a repository by the author(s) or with their consent.

complex shape track [12–14]) and the desired curvature for path tracking, drift equilibria are calculated using simplified vehicle models [15–17] to generate target states (velocity, sideslip, etc.) for the subsequent drift controllers using different control algorithms (i.e. linear quadratic regulator [18], model predictive control [3,19–23] or neural network-based approach [24,25]).

However, for drift-assist control system in the framework of Advanced Driver Assist System (ADAS), which has been introduced in several high-performance vehicles [26–28], a human driver is expected to initiate the drifting behaviour of the vehicle and perform counter steering for path tracking [29]. Without prior path knowledge and preplanned manoeuvres, the first challenge is how to accurately interpret the demand of the human driver to transition between normal driving and drifting, before enabling/disabling the assist controllers that stabilise the high sideslip during drifting with AWD front/rear axle torque distribution [30,31] or four-wheel independent drive torque allocation [29,32].

In previous studies, rule-based conditions are widely applied to activate/deactivate the drift controller in relatively simple scenarios (circular track [33] or U-turn [34]). For example, based on full throttle input, yaw rate and sideslip angle thresholds, ref. [35] develops a rule-based algorithm to activate the drift control. References [12,13,36] utilise the track position of the vehicle to decide the engagement period of the drift controller. Reference [37] sets an open-loop policy to initiate drifting with maximum steering input. Reference [33] deploys a button on the dashboard to allow the driver to turn on the drift mode manually. Reference [34] considers the counter-steering behaviour of a human driver to decide the engagement of drift control. Reference [38] utilises full throttle as a trigger to enable sideslip control until the driver performs counter steering.

To better interpret driver's intention to drift, in order to activate the drift controller intuitively in an unknown environment, this paper explores the topic of drift intention recognition, which is rarely covered in previous research. In fact, driver intention recognition is now playing an important role in the framework of ADAS, for instance, reference [39] proposes a steering control framework in which a lane change path is planned according to the identified driver intention, and in ref. [40], different driving behaviours are identified for vehicle motion prediction related to energy consumption. In general, the task of intention recognition is mostly treated as a classification problem, in which the driver's intention or status is identified as a particular type, to further support subsequent motion planning and control.

Besides rule-based fuzzy logic [41] or machine learning classification approaches like support vector machine (SVM) [42], the methods for driver intention recognition could be generally divided into two types, probabilistic models and neural network-based models [43], and the main application is to detect intentions related to lane changing and turning. For probabilistic models, different nodes are defined to represent different variables or behaviours, and the concerned intention is calculated according to the conditional transition possibilities from related nodes. In ref. [44], to predict lane-changing behaviour, two Bayesian networks (BN) are utilised to interpret nearby lane conditions and driver's gaze behaviour, respectively. In addition to BN, dynamic Bayesian networks (DBN) could additionally consider the state from the previous timestep, resulting in higher accuracy in lane-changing recognition [45]. For the hidden Markov model (HMM), the hidden state

of lane changing could be inferred according to the observed variables including driver inputs and vehicle state data [46].

Despite the success of the above probabilistic models, neural network-based approaches, including artificial neural network (ANN) and recurrent neural network (RNN), have been more preferable in recent years for a higher prediction accuracy [43], as refs [47,48] use ANN, refs [49,50] use RNN, ref. [51] uses gate recurrent unit (GRU), refs [52–55] utilise long short-term memory (LSTM) and ref. [56] uses bidirectional LSTM (Bi-LSTM) with vehicle lateral dynamics features to classify lane changing or keeping. Moreover, ref. [57] proposes a convolutional neural network (CNN) structure to process both visual environmental information and vehicle states. In general, the features that could be used as inputs for neural network-based classification could be concluded into three types [58]: environmental features (i.e. car positions in nearby lanes [59] or GPS map data [55]), driver behaviour (gaze, head position, electroencephalography signals, etc. [49,60,61]) and vehicle dynamics behaviours (yaw rate, lateral velocity [62] and acceleration [63]). Furthermore, visual features related to surrounding traffic scenarios [64–66] and image-based driver information [67–69] could also be directly applied for driver intention or behaviour recognition (distractions, drowsiness, etc.), in order to support a driver-monitoring system and the inputs are normally processed with CNN. However, for the concerned scenario of drifting in this paper, environmental information like lane features may not be available due to the racetrack layout. Besides the driver's face may not be observable when wearing a helmet. Therefore, in this paper, we utilise only steering and pedal inputs from the driver, and readily available vehicle states assuming standard instrumentation as inputs for the drift intention recognition.

In summary, this paper proposes a neural network-based method to recognise the driver's intention to drift, in order to support the engagement of the subsequent drift controller at the desired moment. The contributions of this paper are as follows:

1) In contrast to studies using preplanned manoeuvres or additional inputs like buttons to decide when and where to start drifting, we propose a data-based approach to detect driver's desire to start/exit drifting within 500 ms.
2) Distinct driver input features and acceleration signals during normal/drifting cornering are collected and analysed, respectively, only relying on basic driver inputs (steering and pedals) and vehicle state signals. Two Bidirectional Long Short-Term Memory Network (Bi-LSTM) models are trained separately based on the selected signals for the recognition of the Intention to Start Drifting (ISD) and the Intention to Exit Drifting (IED). The models are trained and evaluated through a data set that contains 525 laps of driving, including 5 different drivers, 35 car models and 2 tracks, collected from the racing simulator Assetto Corsa with realistic physics engine and vehicle models.
3) The generalisation ability of the proposed approach is validated through test sets with different drivers, track layouts and car models. The proposed intention recognition models reach an overall accuracy of 90% and outperform other machine learning methods in recognising the two concerned intentions. Furthermore, the effects of window size and classification weights during model training are further discussed regarding classification accuracy and safety concerns.

Software and hardware configurations

Software platform

In this work, we have selected Assetto Corsa [70] for driver-in-loop simulation and data collection for the following reasons. Firstly, the focus of this work is more about driver's intention and behaviour, so not only a detailed vehicle dynamics model but also a friendly user interface and realistic graphics should be guaranteed. Furthermore, Assetto Corsa is a widely used virtual racing environment for the training of professional drivers [71] like Formula 1 World Champion Max Verstappen [72], with a physics engine to consider detailed modelling of powertrain, suspensions, tyres, etc. Secondly, to enhance the generalisation ability of the trained classifier, in addition to different drivers, a variety of vehicles should be utilised and tested to provide data. Assetto Corsa includes over 100 licenced vehicle dynamics models from manufacturers like Ferrari, Porsche, McLaren, etc., and laser scanning technology is applied in reproducing real-world race tracks.

To export the signals from Assetto Corsa to Matlab for classifier training, Assetto Corsa Telemetry Interface (ACTI) [73] and Motec i2 [74] are used for data extraction and format conversion, respectively.

Hardware platform

The driving simulator of Cranfield University (Figure 1) is adopted as the driver-in-loop platform, which includes a set of surrounding screens, a steering wheel, pedals and a motion feedback seat. To be specific, the surrounding screen could provide a field of view of 180 deg, the Leo Bodnar steering wheel guarantees realistic force feedback with a maximum of 26 Nm, and the two-degree-of-freedom (2DOF) motion feedback seat supports pitch and roll movement. Note that the yaw motion is not available in this setup, the effects of which should be further investigated in future work.

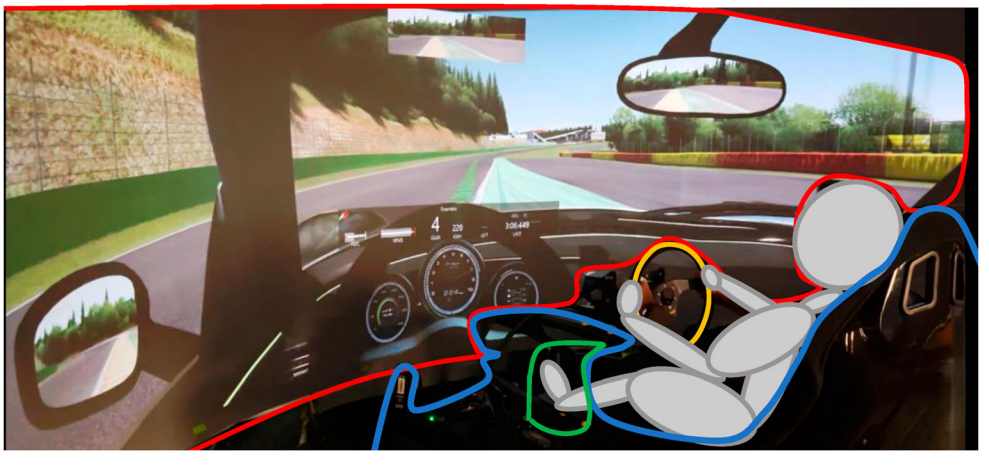


Figure 1. Driving simulator of Cranfield University.

Experiment design for data collection

Test tracks

As shown in Figure 2, data are collected from two tracks. Track 1 and Track 2 have three and two corners, respectively. By plotting the trajectory radius and vehicle speed from a given lap, it can be seen that the trajectory radius (raw value calculated as speed divided by path angle rate, thereby having fluctuations) varies in different tracks and corners. For example, the radius on Track 1 is generally above 40 m, but for Track 2, it is around 20 m. In addition, since the drivers are required to push the vehicle to the adhesion limit, a correlation could be observed between speed and radius (for Track 1, with 40 m radius, the speed is around 20 m/s; for Track 2, with 20 m radius, the speed is around 14 m/s). The aim of using two tracks is to increase the variety of the data and also to improve and validate the generalisation ability of the subsequent intention recognition model against different path geometry, as Track 2 will be used as a test set only.

In both tracks, the drivers are asked to perform Normal Cornering Laps and Drift Cornering Laps separately (Figure 2(a)), and then, the data will be labelled with different behaviours (Normal Corner Entrance, Drift Corner Entrance, etc.). These behaviours will be explained in the following sections.

Test drivers

Five drivers are recruited from Cranfield University (mean age of 27.8 years old with 7.0 years of driving experience, no professional race drivers involved), and the number of participants is limited as advanced driving skills are required in order to provide valid drifting data to train the subsequent intention recognition models. Especially for the second intention (Intention to Exit Drifting, which will be discussed in the following sections), the driver is expected to be able to maintain drifting to generate data regardless of the training set or then the test set. And more participants will be involved in the future when the drift-assist control proposed in our study [29] is integrated with this study in a holistic control framework, so that more inexperienced drivers will be assisted in drifting and therefore be included to further test the model proposed in this paper.

Test vehicles

In total, 35 cars from 16 brands are tested to provide data. Since the focus of this work is driver's intention, no specific powertrain configuration is preferred with the majority of the vehicles being Rear-Wheel-Drive (RWD) and 10 out of the 35 being 4-Wheel-Drive (4WD) (as shown in Table 1). Note that no Front-Wheel-Drive (FWD) vehicles are involved since they cannot be stabilised to a drift equilibrium by power sliding where the rear tyres are saturated at adhesion limit by drive torque [4,16].

Driving tasks for data generation

To generate datasets for both training and testing and subsequently evaluate the generalisation ability of the trained classifier dealing with different drivers and vehicle models, different drivers are allocated with different vehicles (Table 3). For Track 1, each of the five

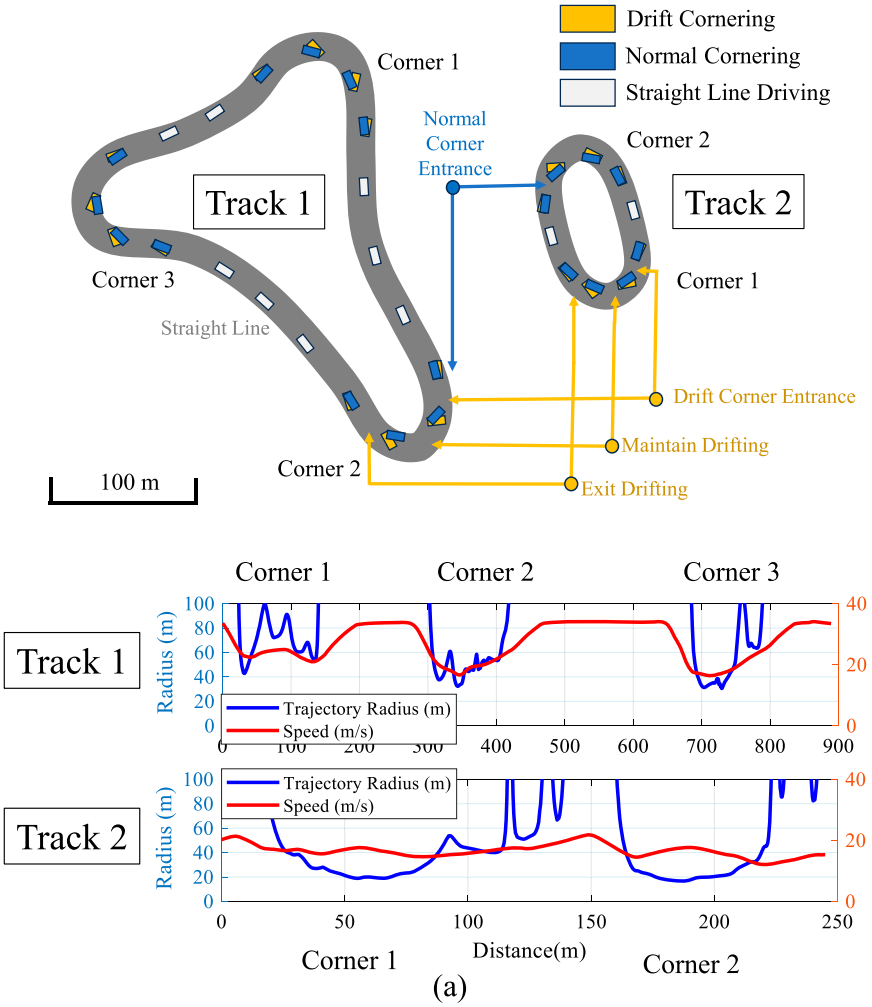


Figure 2. Test tracks and drifting in Assetto Corsa.

Table 1. Drivetrain layout (RWD/AWD) of the test vehicles.

	Number of Vehicle	Number of Lap
RWD	25	420
AWD	10	105
Total	35 vehicles	525 laps

Table 2. Manoeuvres (Drift/Normal Cornering) on test tracks.

	Drift Cornering Lap	Normal Cornering Lap	Total
Track 1	308	205	513
Track 2	6	6	12
Total	314	211	525 laps

Table 3. Drivers, vehicles and tracks information in the data sets.

		Vehicle number	Track number	Laps	Data set
Driver 1		1 ∼ 10 (2AWD)	1	225	Training set
Driver 2		11 ∼ 15 (2AWD)		72	Test set 1
Driver 3		16 ∼ 20 (2AWD)		63	
Driver 4		21 ∼ 25 (2AWD)		66	Test set 2
Driver 5		26 ∼ 32 (1AWD)		87	
Driver 1		33 ∼ 35 (1AWD)	2	12	Test set 3
Total	5 drivers	35 vehicles	2 tracks	525 laps	4 sets

drivers is assigned to 10, 5, 5, 5, and 7 cars, respectively, to provide data of Normal Cornering Lap and Drift Cornering Lap. The data of Driver 1 on Track 1 is used as the Training set; meanwhile, the data from the rest of the drivers are used as Test sets 1 and 2, as shown in Table 3. For Track 2, which is designed to evaluate the generalisation performance of the trained model in different corners and track layouts (Test set 3 in Table 3), only Driver 1 is included with three cars.

The detailed requirements for performing Normal Cornering Lap and Drift Cornering Lap (211 and 314 laps, respectively, as shown in Table 2) are elaborated as follows: In Normal Cornering Lap, the drivers are asked to drive as fast as possible and accelerate through the corner. Specifically, to brake hard in a straight line and carry the throttle through the corners aiming to operate the vehicle near the limit of lateral acceleration, the sideslip should always be low and in the stable region. The purpose behind such a requirement is to develop a model that could precisely perceive the specific difference between Normal Cornering and Drift Cornering, as in both scenarios, the vehicle is operating near the edge of road friction in the presence of high throttle and acceleration. In Drift Cornering Lap, the drivers are asked to perform drifting in the target corners. Only 'power-sliding' drifting is allowed, that is, no shifting or handbraking is involved, thus the driver is likely to apply the throttle in a more abrupt way in the corner to destabilise the rear axle and initiate drifting, followed by counter-steering and cooperation of throttle and steering to maintain drifting.

It should be noticed that we do allow the driver to fail in drifting, for example, the vehicle end in spinning due to the driver applying too much throttle while initiating drifting or untimely counter steering. The data are still used and labelled as discussed in detail in the following sections.

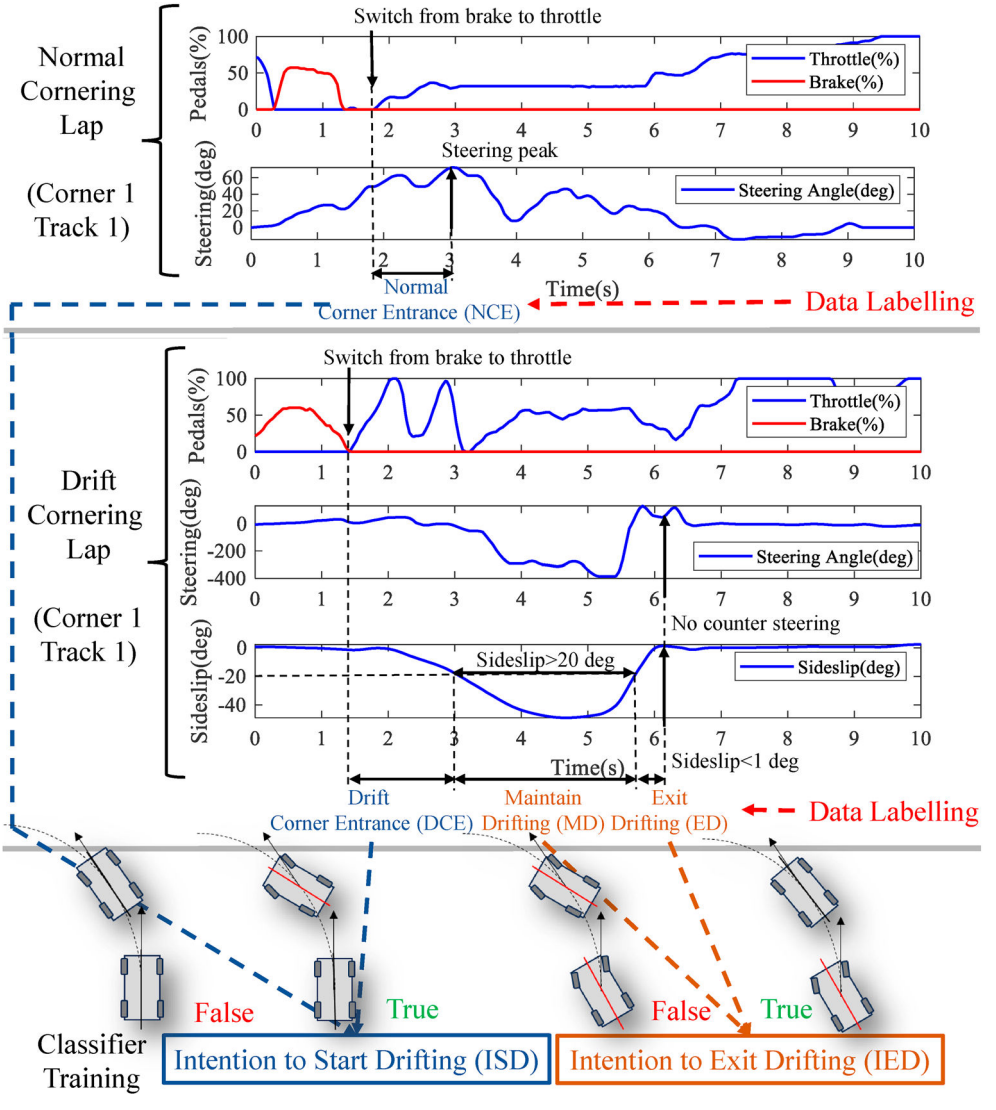


Figure 3. Labelling of data to classify two concerned intentions (ISD and IED).

Data preprocessing and labelling

After data collection, the next step is data labelling before utilising the collected driver and vehicle behaviours for classifier training and intention recognition. In detail, there are two specific intentions to recognise as mentioned: Intention to Start Drifting (ISD) and Intention to Exit Drifting (IED), as shown in Figure 3.

Intention to start drifting (ISD)

For ISD, two types of data are labelled as without/with the ISD for classification, named Normal Corner Entrance (NCE) and Drift Corner Entrance (DCE), respectively:

Normal corner entrance (NCE)

The data are collected from normal driving laps, which start from the timestep when the driver switches from brake to throttle while entering the corners and end when the steering angle reaches peak value and the vehicle passes the apex point of corners.

Technically, what the drivers are encouraged to do in the test does not strictly count as ideal 'race cornering' as the throttle is applied before the apex. The reason behind such instruction to the driver is that the presence of throttle is essential for these two types of data. As the absence of throttle could simply imply that the driver desires no drifting, and the difficulty of the concerned intention recognition task is to understand whether the driver wants to drift through the corner or just wants to raise the cornering speed.

Drift corner entrance (DCE)

The data collected from drift driving laps also starts from the switch from brake to throttle but ends at the timestep when the sideslip is over 20 deg, where the vehicle is regarded to have transitioned into drifting with high sideslip.

Concerns could be raised about selecting 20 deg of sideslip as a condition to divide Drift Corner Entrance and the following behaviours of Maintain Drifting and Exit Drifting (Figure 3). First of all, this value is set according to an observation of the collected data. As shown in the driver inputs plot during Drift Cornering Lap in Figure 3, at the time when sideslip increases over 20 deg, the driver generally starts to perform counter steering, the typical behaviour of drifting. Also, for the exit of drifting, when the sideslip returns below 20 deg, a reduction of throttle could also be observed, which indicates the driver desires to reduce the slip of tyres and end drifting. Furthermore, since we aim to increase the recognition accuracy of the intention to start/exit drifting, we suppose 20 deg is an appropriate value to guarantee enough data volume during drifting initiation and termination.

Moreover, a sideslip of 20 deg is high enough to distinguish drifting for normal cornering, since the maximum sideslip for normal cornering is usually below 10 deg in normal driving due to the 'bifurcation' in vehicle dynamics [1,16,17].

Also, 20 deg of sideslip is a moderate value for drifting considering the stock vehicles we used in this study. According to previous studies [17], the sideslip angle during drifting is strongly and also linearly related to the steering angle (a higher sideslip needs higher counter steering); in ref. [12], a front-wheel steer angle of nearly 40 deg to maintain drifting at 40 deg sideslip using a modified vehicle. However, for most of the stock vehicles in our dataset, the maximum wheel steering angle is significantly lower than 40 deg (i.e. the maximum steering angle for Ferrari LaFerrari is about 30 deg); therefore, drifting is achieved at lower sideslip angles.

Intention to exit drifting (IED)

For IED, similarly, two types of data are labelled as without/with IED for classification, named Maintain Drifting (MD, without IED) and Exit Drifting (ED, with IED).

It should be noticed that no data from Normal Cornering Lap is utilised for this classifier training. To determine if the driver intends to maintain or exit drifting, the training data must be gathered during drifting or exiting a drift. Neither of these behaviours occurs during a Normal Cornering Lap. Consequently, only the data from Drifting Cornering Lap is utilised (as shown in Figure 3). Moreover, to train the classifier to distinguish between

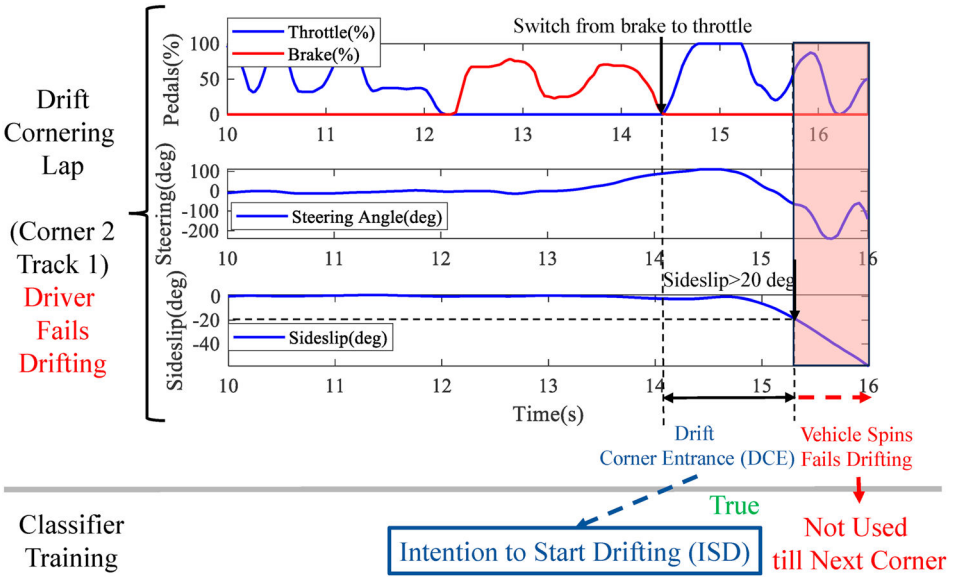


Figure 4. Labelling of data when the driver fails in drifting.

two behaviours, the initial state of the prepared data should be similar or nearly the same, thus for both MD and ED, the data start from a sideslip angle in drifting at 20 deg (bottom plot in Figure 3).

Maintain drifting (MD)

During drift cornering laps, for the time period when the sideslip is continuously above 20 deg, it is supposed that the driver desires to maintain a high sideslip and keep drifting.

Exit drifting (ED)

In drift laps from the timestep when the driver reduces the sideslip to below 20 deg, to the timestep when the sideslip is below 1 deg with no counter steering, the driver's desire during this period is regarded as ED to transition back to normal driving.

Concerns about failed tests

Concerns could be raised on how we process and label the data if the driver fails to maintain drifting and the vehicle ends up spinning. Or what if drifting cannot be initiated due to the understeering nature of some cars? For the first case, taking Corner 2 from one of the laps as an example, as shown in Figure 4, the data will be used for the recognition of ISD, which will be labelled as DCE till the timestep when the sideslip reaches 20 deg. And the data afterwards will be abandoned and not count for the IED classification. For the second case, when the vehicle has an understeering response and fails to start drifting, similarly, the data will only be used for the recognition of ISD and labelled as DCE till the timestep when the driver gives up the throttle in order to bring the vehicle back to track from understeering.

Signals selection for classification and intention recognition

With the aforementioned four types of labelled data to recognise two intentions, in this section, we discuss what signals are used and how we process them before using them as inputs for classifier training and intention recognition. In general, two types of signals are considered and utilised as inputs: driver inputs and vehicle states.

Driver inputs

For driver inputs, not only the throttle position γ and steering wheel angle δ are considered but also their rate $\dot{\gamma}$, $\dot{\delta}$, mean γ_{avg}, δ_{avg} and variance value γ_{var}, δ_{var} in a moving time window are included. The design is due to the driving skills required to perform drifting, especially power sliding in the context of this study, that the driver is expected to destabilise the rear axle with a high slip ratio using throttle, followed by a subtle coordination of throttle and counter steering [4].

In the following discussion sections, the demonstrated driver inputs data are collected from Driver 1 during NCE and DCE on Track 1 (all three corners included).

Driver inputs related to ISD

As shown in Figure 5, in the first 1 s of DCE, compared to NCE, to initiate drifting, the driver tends to apply throttle in a very abrupt way (Figure 5(a)) in order to destabilise the rear axle for high sideslip, followed by an oscillation in the throttle input (Figure 5(b and c)) in order to prevent the vehicle from spinning (sideslip increasing too fast) or returning back to normal cornering. Also, there is an apparent distinction in the steering wheel angle that a counter steering could be observed for DCE as shown in Figure 5(d).

Driver inputs related to IED

As shown in Figure 6(a), though, in general, the throttle is higher in ED due to exiting corners and accelerating on the straight line, an oscillation exists in both MD and ED behaviours, irrespective of the target being to maintain a high sideslip or to reduce the sideslip back to normal driving. Therefore, it is unlikely to use the throttle signals solely to achieve the detection of the IED. As for the steering, for ED, as shown in Figure 6(b), a reverse process of counter steering could be observed, while for MD, there is a continuous counter steering. Such difference in steering behaviour could also be reflected in the steering angular rate (Figure 6(c)) and the variance of steering angle (Figure 6(d)) that for ED, both the steering rate and the variance are higher.

Vehicle states

For vehicle states, we only consider two parts: (1) vehicle yaw rate r, its corresponding derivative $\dot{r}$, moving mean r_{avg} and variance r_{var}; (2) longitudinal/lateral acceleration signals a_x, a_y, their corresponding moving mean a_{xavg}, a_{yavg} and variance a_{xvar}, a_{yvar}.

Note that no velocity signals are involved as inputs for classification, because based on our drift equilibrium analysis [29], drifting could be performed at different trajectory radii, where the steady-state speed will vary accordingly [16,17]. To be specific, drifting is a manoeuvre at the handling limit where the tyre forces are near saturation [5,16], so the

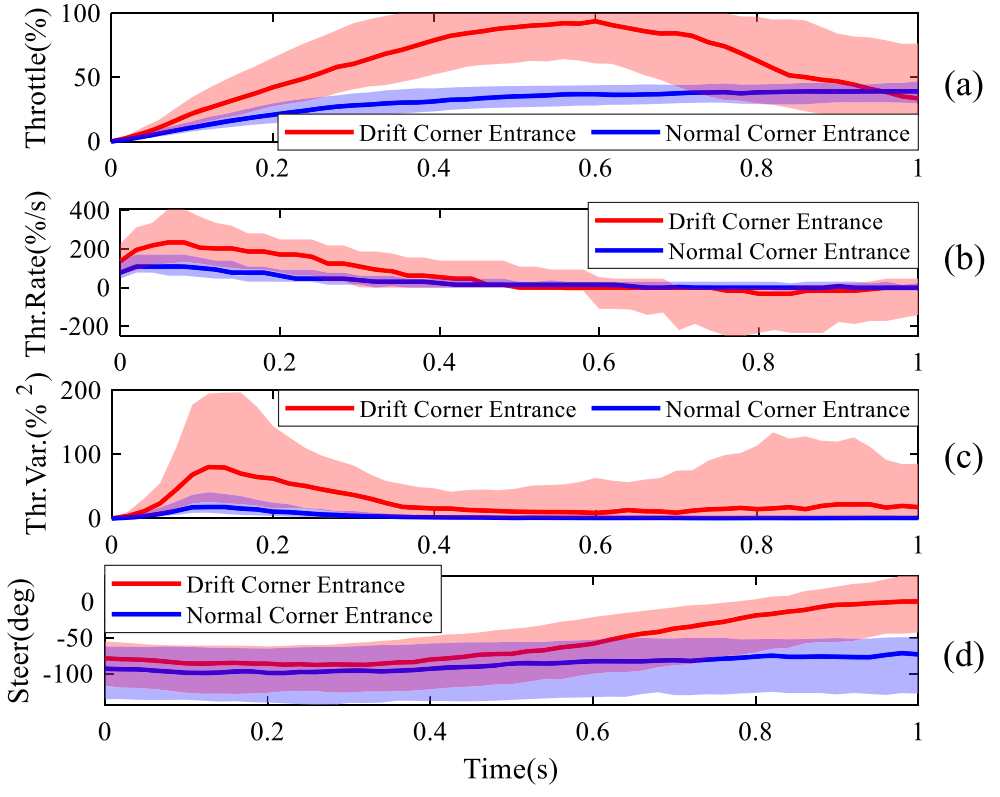


Figure 5. Driver inputs comparison (median value and interquartile range) between Drift Corner Entrance (DCE) and Normal Corner Entrance (NCE), for Intention to Start Drifting (ISD) recognition.

acceleration during drifting will generally follow the adhesion limit of the road, regardless of the radius of the corner. In addition, with a given acceleration, the speed at drift equilibrium will highly depend on the trajectory radius. Therefore, to ensure the generalisation ability of the classifier in different tracks, we chose to ignore the speed signals. In addition, the speed also needs estimation in reality, particularly in drifting with high tyre slip [4].

As for the yaw rate, we include it since it reflects the transient-state vehicle behaviour during the entry/exit of drifting. Specifically, the yaw rate includes both the path angle rate (which decides the vehicle trajectory) and the sideslip rate (affects the sideslip during drifting) [12,18], with the latter being the key difference between normal cornering and drifting.

In the following discussion sections, the demonstrated vehicle states data are collected from Driver 1 during NCE and DCE on Track 1 (all three corners included).

Vehicle states related to ISD

For ISD, the distinct behaviours of NCE and DCE are shown in Figure 7. As a consequence of the abrupt throttle input to start drifting, the longitudinal acceleration of DCE is higher (Figure 7(a)), which also contributes more to the total centripetal acceleration when the sideslip increases. The variance of longitudinal acceleration is also higher as shown in Figure 7(b). Due to the increased sideslip and longitudinal acceleration contributing more

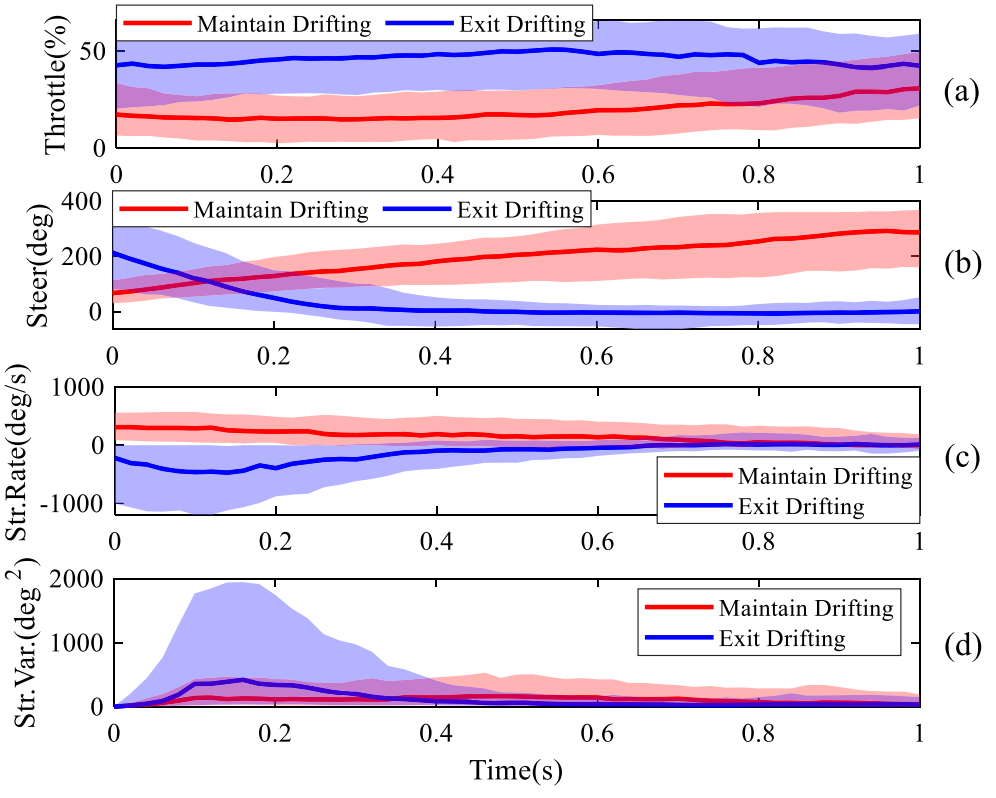


Figure 6. Driver inputs comparison (median value and interquartile range) between Maintain Drifting (MD) and Exit Drifting (ED), for Intention to Exit Drifting (IED) recognition.

to the centripetal acceleration, also the saturated tyre force during drifting [5,16], the lateral acceleration during DCE is slightly lower (negative value due to right-hand corner) compared to NCE (Figure 7(c)). In Figure 7(d), we observe the yaw rate in DCE increasing to higher magnitudes (negative value due to right-hand corner) in order to generate a high sideslip for drifting (clock wisely rotates the vehicle 'deeper' towards the corner). With this instance, we recall the relationship between the yaw rate and the sideslip rate in drifting [12,18]. Consequently, more fluctuation could also be observed from the rate of yaw rate in Figure 7(e).

Vehicle states related to IED

For IED, as shown in Figure 8(a), reducing sideslip while returning to straight-line driving comes along with a clear reduction in lateral acceleration (negative). The variance of the lateral acceleration during the transient phase of ED is also higher (Figure 8(b)) compared to the nearly steady-state MD phase. Furthermore, the longitudinal acceleration during ED is higher as shown in Figure 8(c), as the drivers accelerate while exiting the corner. In addition, due to the reduction of sideslip in ED, and the relationship between the sideslip and yaw rates as discussed in the previous section, more fluctuation could be observed in the rate and variance of yaw rate for ED in Figure 8(d and e).

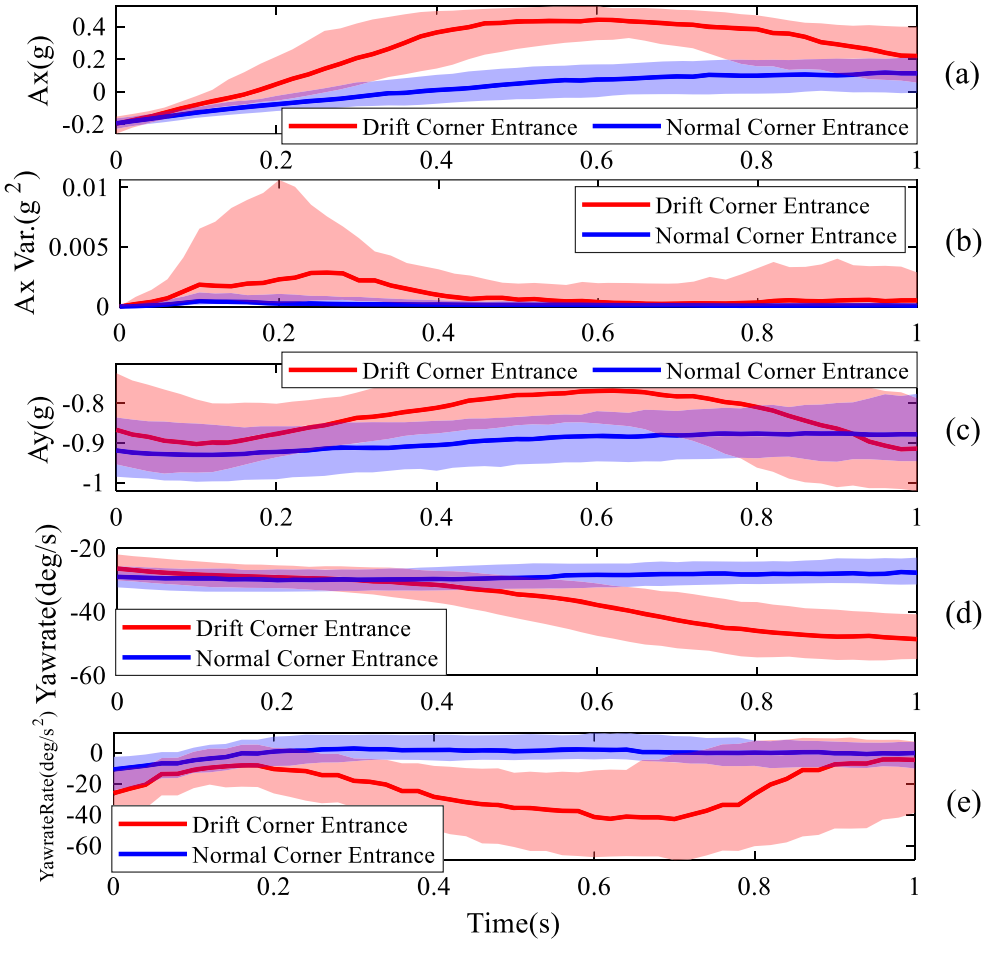


Figure 7. Vehicle acceleration signals comparison (median value and interquartile range) between Drift Corner Entrance (DCE) and Normal Corner Entrance (NCE), for Intention to Start Drifting (ISD) recognition.

Model training

Input signals for classification model

With the selected signals, the data vector $\boldsymbol{x}_k$ generated at timestep k for classification could be written as (1).

$$\begin{aligned}\boldsymbol{x}_k = [&\delta_k, \dot{\delta}_k, \delta_{\text{avg}_k}, \delta_{\text{var}_k}, \gamma_k, \dot{\gamma}_k, \gamma_{\text{avg}_k}, \gamma_{\text{var}_k},\\ &a_{x_k}, a_{\text{xavg}_k}, a_{\text{xvar}_k}, a_{y_k}, a_{\text{yavg}_k}, a_{\text{yvar}_k}, , r_k, \dot{r}_k, r_{\text{avg}_k}, r_{\text{var}_k}]\end{aligned} \tag{1}$$

After selecting the input signals for classification, the sample frequency and window size of the signals should be discussed. We consider a sample frequency of 10 Hz ($\Delta t = 0.1\ s$) to suit the sensors on a production vehicle. Taking the window size of 0.5 s for instance, the input vector $\boldsymbol{X}$ at timestep k for classification training can be expressed as (2).

$$\boldsymbol{X}_k = [\boldsymbol{x}_{k-5}, \ldots, \boldsymbol{x}_k] \tag{2}$$

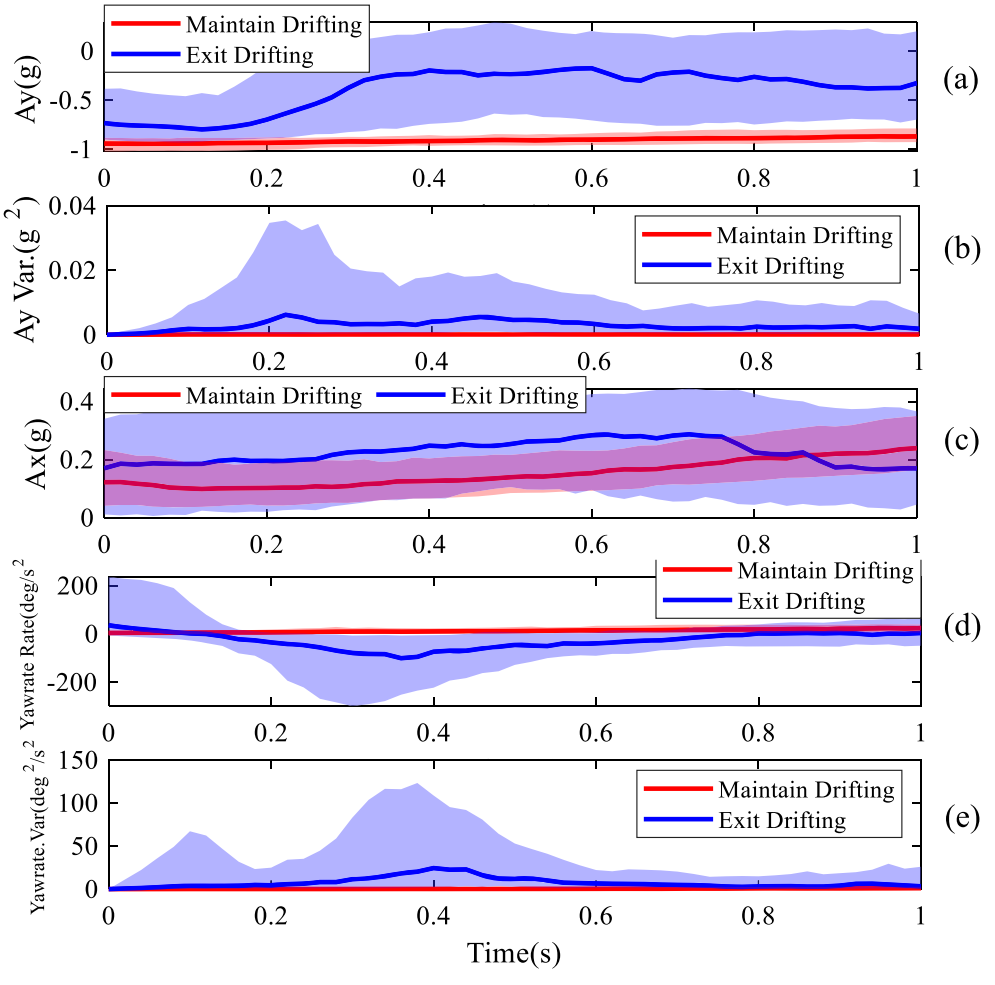


Figure 8. Vehicle acceleration signals comparison (median value and interquartile range) between MD and ED, for Intention to Exit Drifting (IED) recognition.

Structure of the applied Bi-LSTM network

As discussed in the introduction section, ANN- and RNN-based approaches have been widely applied in recent years for a higher prediction accuracy [43] (i.e. ANN [47,48], GRU [51], LSTM [52–55], Bi-LSTM [56]). In this paper, we apply Bi-LSTM as it comprehensively considers data sequence in both forward/backward directions (unlike LSTM only processes one direction), leading to improved accuracy in time-series classification [75]. Also, LSTMs hold the advantage in dealing with long-range dependencies when compared with GRU [76]. In addition, Bi-LSTM as a type of RNNs can better process sequential data when compared with ANN [77] or SVM [78], therefore is more suitable for the time-series analysis in our study.

The structure of the Bidirectional LSTM (Bi-LSTM) network is demonstrated in Figure 9, which generally contains three main layers: input layer, hidden layer (Bi-LSTM) and output layer. Specifically, the hidden Bi-LSTM layer contains a forward layer and a backward

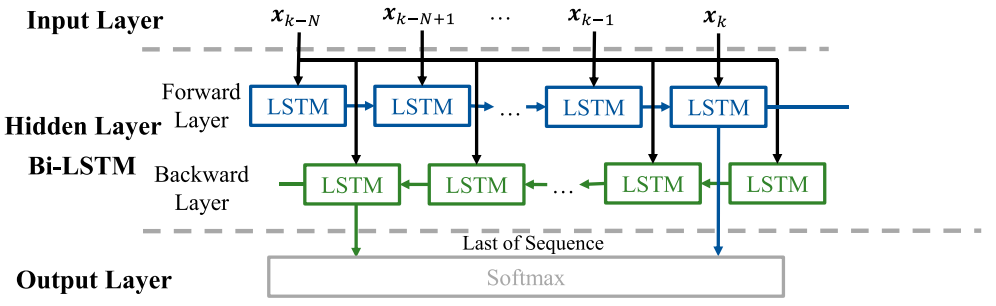


Figure 9. Structure of the Bi-LSTM.

layer, to better comprehend the target behaviour across different timesteps. The inputs for the network are shown in (2), and the Bi-LSTM layer here has 128 units. For each of the two intentions (ISD and IED), a Bi-LSTM is trained independently according to data from the labelled behaviours. Specifically, data from NCE and DCE (Figure 3) are used to train the Bi-LSTM network for the recognition of ISD, and data from MD and ED are used to train the network for the recognition of IED.

Dataset for training and testing

To train the above networks, as shown in Table 3, we only involve the data provided by Driver 1 and Car 1 ~ 10 as a training set, and the data from the other drivers, cars and tracks as testing sets. In detail, Test Set 1 and Test Set 2 are used to evaluate the generalisation of the model with different drivers and car models, and Test Set 3 aims specifically at the recognition performance in unknown tracks, also with additional cars.

Training process

Using the Adam (Adaptive Moment Estimation [79]) optimiser as a solver (batch size of 64, 10 epochs, with cross-entropy loss (3) [80]), the training progress of the Bi-LSTM networks for the two intentions are as follows in Figures 10 and 11.

In detail, as for the cross-entropy loss [80] with N samples, it could be written as (3) where y_i is the true value of the i th sample ($y_i \in \{0, 1\}$ for our binary classification task), $\hat{y}_i$is the predicted probability that the i th sample belongs to the first class ($\hat{y}_i \in [0, 1]$), and w_0, w_1 are the weights for the two classes. Note that the weight setting should consider the balance of positive/negative samples in the dataset, so with N_0 and N_1 samples from two classes, our default setting is to calculate their weight inversely proportional to their frequency in the training data, as shown in (4).

$$Loss = -\frac{1}{N}\sum_{i=1}^{i}[w_0 \cdot y_i \cdot \log(\hat{y}_i) + w_1 \cdot (1 - y_i) \cdot \log(1 - \hat{y}_i)] \tag{3}$$

$$w_0 = \frac{N}{2 \cdot N_0}, w_1 = \frac{N}{2 \cdot N_1} \tag{4}$$

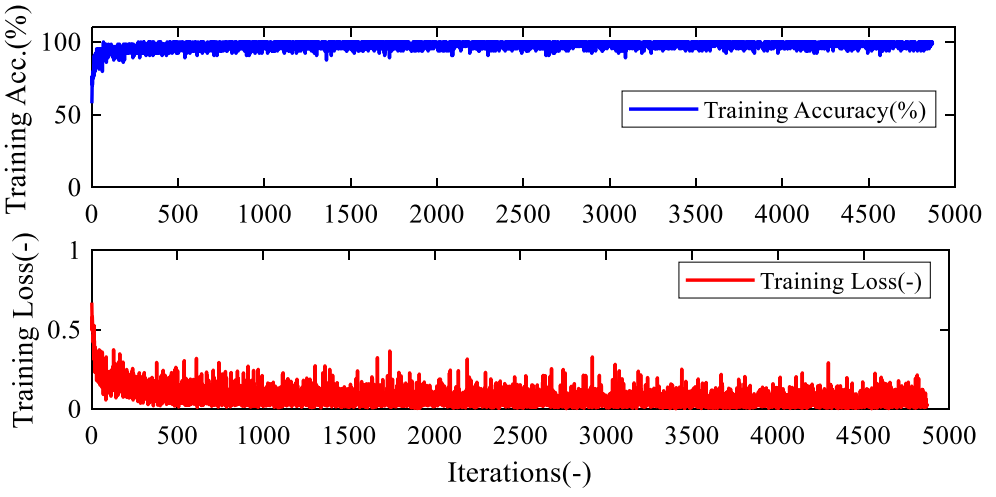


Figure 10. Bi-LSTM training progress for Intention to Start Drifting (ISD) recognition.

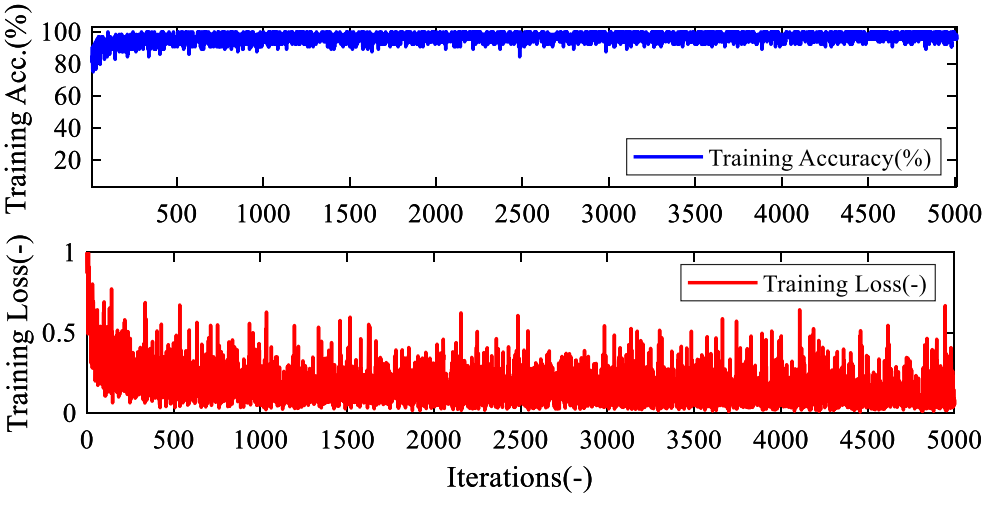


Figure 11. Bi-LSTM training progress for Intention to Exit Drifting (IED) recognition.

For both IED and ISD, as shown in Figures 10 and 11, the models could learn to distinguish driver's intentions in about 1000 iterations (about 2 epochs) that the training accuracy reaches a platform and the training loss reduces to near zero.

Results and discussion

Accuracy results and comparisons

The first and most important metric to evaluate the performance of the intention recognition model is the accuracy, and both the results of the training set and the test set should be discussed. Except from the training set based on the data provided by Driver 1 on Track

Table 4. Accuracy of the Bi-LSTM models to recognise the Intention to Start Drifting (ISD) and the Intention to Exit Drifting (IED).

	Training Set	Test Set 1	Test Set 2	Test Set 3
ISD	99.2%	97.4%	95.7%	91.3%
IED	98.8%	94.5%	89.9%	92.2%

1, the rest of the data is divided into three test sets, as shown in Table 3, to prove the generalisation ability of the model.

In the following sections, we first discuss the ISD/IED recognition accuracy of the proposed Bi-LSTM models and then compare the results with LSTM, GRU, ANN and Second-Order SVM approaches. Note that for the other NNs discussed for comparison, we are using the same inputs (as shown in (2)), the same frameworks (3 main layers as shown in Figure 9) and the same training settings. The only difference is we replace the Bi-LSTM layer in Figure 9 with layers from the other networks (LSTM layer, GRU layer, etc.) for comparison. And the number of hidden units remains the same as 128.

Accuracy of the Bi-LSTM models to recognise ISD and IED

For the recognition accuracy of ISD and IED, the results from the proposed Bi-LSTM models are demonstrated in Table 4, where the selected signals (2) from a window size of 500 ms are used as inputs. The training accuracy is notably high for both intentions (ISD: 99.2%, IED: 98.8%), while a general decline is observed across the three test sets, with ISD ranging from 97.4% on Test Set 1 to 91.3% on Test Set 3, and IED varying from 94.5% to 89.9%. Overall, the results indicate that the Bi-LSTM models are capable of reliably detecting driver intentions related to drifting, with slightly more robustness in identifying ISD compared to IED.

ISD accuracy comparison with other methods

The ISD recognition accuracy of the Bi-LSTM model is compared with other approaches in Table 5. In general, RNN-based (LSTMs, GRU) approaches perform better compared to ANN and SVM, since they are more suitable for the time-series analysis in our study. Compared to the other methods, the Bi-LSTM model has the highest accuracy in all the three test sets, that all the accuracies are above 91%. For Test Sets 1 and 2, all of the methods show a good ability of generalisation that the accuracy could still maintain about 95% while facing different driver and vehicle models. However, For Test Set 3 with a different Track 2, most of the listed approaches suffer from a certain degree of reduction in the recognition accuracy to about 88%, with Bi-LSTM being the only exception. The latter can be explained by the structure of Bi-LSTM, which can better comprehend sequential data in both forward and backward directions and therefore provides better results than the other methods (reason as discussed in the section of Structure of the applied Bi-LSTM network).

IED accuracy comparison with other methods

The IED recognition accuracy of the Bi-LSTM model is compared with other approaches in Table 6. The RNN-based approaches (LSTMs and GRU) still have the advantage in all the test sets, an accuracy of about 90% could be observed with different drivers (Test Set 1, 2) and different track layouts (Test Set 3). In addition, the Bi-LSTM generally outperforms

Table 5. Accuracy of the model to identify the Intention to Start Drifting (ISD).

ISD	Training Set	Test Set 1	Test Set 2	Test Set 3
Bi-LSTM	99.2%	97.4%	95.7%	91.3%
LSTM	99.1%	97.2%	94.5%	89.1%
GRU	98.8%	97.2%	94.7%	89.2%
ANN	98.9%	94.9%	94.7%	87.1%
Second-Order SVM	98.1%	95.9%	94.4%	87.5%

Table 6. Accuracy of the model to identify the Intention to Exit Drifting (IED).

IED	Training Set	Test Set 1	Test Set 2	Test Set 3
Bi-LSTM	98.8%	94.5%	89.9%	92.2%
LSTM	97.3%	93.7%	88.2%	91.6%
GRU	97.8%	93.9%	89.3%	91.2%
ANN	98.9%	93.5%	86.2%	89.1%
Second-Order SVM	98.1%	93.6%	85.4%	87.9%

Table 7. The effect of window size on recognition accuracy of the Intention to Start Drifting (ISD).

ISD	Training Set	Test Set 1	Test Set 2	Test Set 3
Bi-LSTM (100 ms)	93.7%	94.1%	90.4%	83.0%
Bi-LSTM (200 ms)	96.1%	94.9%	91.4%	84.7%
Bi-LSTM (300 ms)	97.8%	95.7%	91.0%	88.4%
Bi-LSTM (400 ms)	98.6%	95.7%	92.5%	88.3%
Bi-LSTM (500 ms)	99.2%	97.4%	95.7%	91.3%

Table 8. The effect of window size on recognition accuracy of the Intention to Exit Drifting (IED).

IED	Training Set	Test Set 1	Test Set 2	Test Set 3
Bi-LSTM (100 ms)	95.6%	91.9%	87.1%	88.8%
Bi-LSTM (200 ms)	96.2%	92.5%	87.8%	89.9%
Bi-LSTM (300 ms)	97.7%	92.1%	88.7%	91.5%
Bi-LSTM (400 ms)	98.3%	93.3%	89.5%	92.0%
Bi-LSTM (500 ms)	98.8%	94.5%	89.9%	92.2%

all the other methods, and we assume that the higher accuracy is caused by the structure of Bi-LSTM when dealing with sequential data as discussed in previous sections.

Effects of input signals window size on classification accuracy

To explore the effects of signal window size on classification accuracy, with all other settings remaining the same, the window size of the signals is varied from 100 ms to 500 ms. The window size is not increased further due to the limited length of the part of the labelled data. The results are shown in Tables 7 and 8.

Effect of window size on ISD accuracy

Firstly, for ISD, it could be concluded that the classification accuracy has an obvious dependency on the window size, by increasing the window size from 100 ms, a gradual improvement in the accuracy could be observed in the Training Set and the Test Sets as well. Especially for Test Set 3, the accuracy increases from 83.0% to 91.3%, which means

Table 9. The confusion matrix for two cases.

		Actual Value	
ISD		DCE (ISD True)	NCE (ISD False)
Predicted Value	DCE (ISD True) NCE (ISD False)	True Positve(TP) False Negative(FN)	False Positive(FP) True Negative(TN)
		Actual Value	
IED		ED (IED True)	MD (IED False)
Predicted Value	ED (IED True) MD (IED False)	True Positve(TP) False Negative(FN)	False Positive(FP) True Negative(TN)

narrowing the window size will significantly harm the performance of the model in different tracks. The window size should be set at no less than 300 ms as the reduction from 300 ms to 200 ms will lead to a noticeable loss in the accuracy for Test Set 3.

Effect of window size on IED accuracy

In contrast, for IED (Table 8), we observe that the window size only has limited contribution. The reduction of window size from 500 ms to 100 ms only leads to a reduction of about 3% in the accuracy for both the Training and Test Sets.

Safety concerns and loss function modifications

Besides the accuracy, another important metric to evaluate the model is the confusion matrix [81], which provides a tabulated summary of actual versus predicted classifications. Such evaluation is crucial in our case, for instance, when the actual desire from the driver is NCE but misclassified as DCE the subsequent drift control would be wrongly activated, causing the vehicle to be destabilised against the driver's expectation. Similar safety concerns could also be raised when the driver demands ED but is misunderstood as MD. Therefore, the False Positive (FP) rate for ISD and the False Negative (FN) rate for IED in Table 9 should be lowered by adjusting the weights (4) in loss function (3) during training. Specifically, we increase the weight of NCE (ISD false) and ED (IED true) for the two cases.

For ISD, we modify the weight of NCE from $w_{\mathrm{NCE}} = \frac{N}{2 \cdot N_{\mathrm{NCE}}}$ in (4) to $w_{\mathrm{NCE}} = \frac{3N}{2 \cdot N_{\mathrm{NCE}}}$, with the weight of DCE remaining the same to (4) as $w_{\mathrm{DCE}} = \frac{N}{2 \cdot N_{\mathrm{DCE}}}$. The results after weight modification are shown in Table 10, where the risk of the concerned misclassification is reduced. Take Test Set 3 as an instance, the percentage of FP is reduced from 6.0% to 3.2%; meanwhile, the FN increases from 2.7% to 6.0%, and the total accuracy also slightly drops from 91.3% to 90.8%. In addition, the metric of true negative rate (TN/(TN + FP)) is also useful for this case that for Test Set 3, it increases from 88.7% to 94.0% after the modification of the weights. Similar tendencies could also be observed from the other data sets that there is a trade-off between FP and FN, and a loss of total accuracy when we prioritise ISD False (NCE) due to the previous concern.

For the second intention of IED, similar to the previous case, we modify the weight of ED from $w_{ED} = \frac{N}{2 \cdot N_{ED}}$ in (4) to $w_{ED} = \frac{3N}{2 \cdot N_{ED}}$, with the weight of MD remaining the same to (4) as $w_{MD} = \frac{N}{2 \cdot N_{MD}}$. The results are shown in Table 11, the default weight setting (4) for classification will cause safety concerns for Test Set 2, as the FN rate is 8.3% (8.3% of ED are wrongly classified as MD). After the weight modification, such risk is reduced to

Table 10. ISD confusion matrix after adjusting the weights in the loss function.

Overall Accuracy & Confusion Matrix	Training Set	Test Set 1	Test Set 2	Test Set 3
Default Weight (4)	99.2% 55.0% 0.3% 0.5% 44.2%	97.4% 46.6% 2.0% 0.6% 50.7%	95.7% 45.1% 3.3% 1.0% 50.6%	91.3% 44.1% 6.0% 2.7% 47.2%
Modified Weight	99.1% 54.7% 0.1% 0.8% 44.4%	97.2% 45.5% 1.1% 1.7% 51.6%	94.1% 42.1% 1.9% 4.0% 52.0%	90.8% 40.8% 3.2% 6.0% 50.0%

Table 11. IED confusion matrix after adjusting the weights in the loss function.

Overall Accuracy & Confusion Matrix	Training Set	Test Set 1	Test Set 2	Test Set 3
Default Weight (4)	98.8% 29.7% 0.3% 0.9% 69.1%	94.5% 31.6% 2.3% 3.2% 62.9%	89.9% 29.6% 1.8% 8.3% 70.3%	92.2% 36.0% 5.8% 2.0% 56.2%
Modified Weight	97.0% 30.2% 2.6% 0.4% 66.8%	93.3% 32.8% 4.7% 2.0% 60.5%	86.3% 36.0% 11.8% 1.9% 60.3%	88.6% 36.7% 10.1% 1.3% 51.9%

1.9%, while for the other two Test Sets, the FN rates after modification are also below 2.0%. Besides, the metric of recall (TP/(TP + FN)), which suits this case, increases significantly from 78.1% to 95.0% for Test Set 2. Similar to the previous case, the cost of this modification is a drop in the total accuracy.

Conclusions

To support the development of the drift-assist control system, it is necessary to be able to interpret the driver's intention to drift at the desired moment. In this paper, we propose a data-based approach based on Bi-LSTM to detect driver's intention to start/exit drifting, only relying on driver inputs and vehicle state signals. According to the data collected from various drivers, vehicle models and track layouts in the Assetto Corsa simulation software, we firstly discussed the distinctive driver behaviours in throttle, steering and the corresponding acceleration signals during normal cornering and drifting cornering laps. Then, based on the selected signals and a window size of 500 ms, two Bi-LSTM models were trained separately for the recognition of the 'Intention to Start Drifting' (ISD) and the 'Intention to Exit Drifting' (IED). To validate the generalisation ability and robustness of the proposed approach, different test sets of different drivers, vehicle models and tracks are utilised; the proposed intention recognition models successfully reached an accuracy of over 90% in recognising the two intentions and outperformed other machine learning classification methods in comparison, due to the advantage in the network structure of Bi-LSTM dealing with time-series data. Furthermore, the effects of window size and

classification weights during model training were further discussed regarding classification accuracy and safety concerns according to the misclassification possibilities in the confusion matrix.

Limitations and future work

For the software and hardware configurations in this study, yaw motion feedback is not available in the setup, and the effects should be further evaluated through real-world data in future work. Also, for the number of participants, it is limited in this paper due to the driving skill required for drifting.

Further investigation to analyse the effects of different inputs (vehicle states and driver inputs) on the classification accuracy and the generalisation ability of the trained model. Also, inputs like environment information should be further considered if available. Various scenarios should be tested well for a holistic discussion.

As for the methods to be applied for classification, more advanced algorithms should be involved, with the effects of the algorithm together with the loss function, and the solver should be further investigated. More metrics should also be introduced for detailed analysis as well.

Most importantly, the proposed system should be further tested after the integration with our drift-assist control concept proposed in [29], and those inexperienced drivers could also be included to further test the model proposed in this paper.

Acknowledgments

The financial and intellectual contributions of Rimac Technology are acknowledged for their role in supporting this research.

Disclosure statement

No potential conflict of interest was reported by the author(s).

Funding

This work was supported by the Rimac Technology.

References

[1] Ono E, Hosoe S, Hoang DT, et al. Bifurcation in vehicle dynamics and robust front wheel steering control. IEEE Trans Control Syst Technol. 1998;6(3):412–420. doi:10.1109/87.668041

[2] Xie Z, Ramezani M, Levinson D. Reduced-scale mobile robots for autonomous driving research. IEEE Trans Intell Transp Syst. 2024;25(11):15367–15387. doi:10.1109/TITS.2024.3426508

[3] Stano P, Tavernini D, Montanaro U, et al. Enhanced active safety through integrated autonomous drifting and direct yaw moment control via nonlinear model predictive control. IEEE Trans Intell Veh. 2024;9(2):4172–4190. doi:10.1109/TIV.2023.3340992

[4] Abdulrahim M. On the dynamics of automobile drifting; 2006. [Online]. https://doi.org/10.4271/2006-01-1019.

[5] Edelmann J, Plöchl M, Lugner P, et al. Investigations on the powerslide of automobiles. In: Proceedings of AVEC'08; 2008.

[6] Edelmann J, Plöchl M. Handling characteristics and stability of the steady-state powerslide motion of an automobile. Regul Chaotic Dyn. 2009;14(6):682–692. doi:10.1134/S1560354709060069
[7] Liaw DC, Chiang HH, Lee TT. Elucidating vehicle lateral dynamics using a bifurcation analysis. IEEE Trans Intell Transp Syst. 2007;8(2):195–207. doi:10.1109/TITS.2006.888598
[8] Velenis E, Katzourakis D, Frazzoli E, et al. Steady-state drifting stabilization of RWD vehicles. Control Eng Pract. 2011;19(11):1363–1376. doi:10.1016/j.conengprac.2011.07.010
[9] Velenis E, Frazzoli E, Tsiotras P. Steady-state cornering equilibria and stabilisation for a vehicle during extreme operating conditions. Int J Veh Auton Syst. 2010;8:217–241. doi:10.1504/IJVAS.2010.035797
[10] Baur M, Bascetta L. An experimentally validated LQR approach to autonomous drifting stabilization. In: 2019 18th European Control Conference (ECC); 25-28 June 2019; 2019. p. 732–737.
[11] Goh JY, Gerdes JC. Simultaneous stabilization and tracking of basic automobile drifting trajectories. In: 2016 IEEE Intelligent Vehicles Symposium (IV); 19-22 June 2016; 2016. p. 597–602.
[12] Goh JY, Goel T, Christian Gerdes J. Toward automated vehicle control beyond the stability limits: drifting along a general path. J Dyn Syst Meas Contr. 2020;142(2):021004. doi:10.1115/1.4045320
[13] Acosta Reche M, Kanarachos S, Fitzpatrick M. A hybrid hierarchical rally driver model for autonomous vehicle agile maneuvering on loose surfaces. In: presented at the International Conference on Informatics in Control, Automation and Robotics; 2017.
[14] Baars M, Hellendoorn H, Alirezaei M. Control of a scaled vehicle in and beyond stable limit handling. IEEE Trans Veh Technol. 2021;70(7):6427–6437. doi:10.1109/TVT.2021.3085503
[15] Velenis E, Frazzoli E, Tsiotras P. On steady-state cornering equilibria for wheeled vehicles with drift. In: Proceedings of the 48h IEEE Conference on Decision and Control (CDC) held jointly with 2009 28th Chinese Control Conference; 15-18 Dec. 2009; 2009. p. 3545–3550.
[16] Hindiyeh RY, Gerdes JC. Equilibrium analysis of drifting vehicles for control design; 2009. [Online]. https://doi.org/10.1115/DSCC2009-2626.
[17] Voser C, Hindiyeh RY, Gerdes JC. Analysis and control of high sideslip manoeuvres. Veh Syst Dyn. 2010;48:317–336. doi:10.1080/00423111003746140
[18] Hindiyeh RY, Christian Gerdes J. A controller framework for autonomous drifting: design, stability, and experimental validation. J Dyn Syst Meas Contr. 2014;136(5):051015. doi:10.1115/1.4027471
[19] Hu C, Zhou X, Duo R, et al. Combined Fast Control of Drifting State and Trajectory Tracking for Autonomous Vehicles Based on MPC Controller. In: 2022 International Conference on Robotics and Automation (ICRA); 23–27 May 2022; 2022. p. 1373–1379.
[20] Chen G, Zhao X, Gao Z, et al. Dynamic drifting control for general path tracking of autonomous vehicles. IEEE Trans Intell Veh. 2023;8(3):2527–2537. doi:10.1109/TIV.2023.3235007
[21] Guo H, Tan Z, Liu J, et al. MPC-based steady-state drift control under extreme condition. In: 2021 33rd Chinese Control and Decision Conference (CCDC); 22–24 May 2021; 2021. p. 4708–4712.
[22] Dong H, Yu H, Xi J. Real-time model predictive control for simultaneous drift and trajectory tracking of autonomous vehicles. In: 2022 6th CAA International Conference on Vehicular Control and Intelligence (CVCI); 28-30 Oct. 2022; 2022. p. 1–6.
[23] Goh JYM, Thompson M, Dallas J, et al. Beyond the stable handling limits: nonlinear model predictive control for highly transient autonomous drifting. Veh Syst Dyn. 2024;62(10):2590–2613. doi:10.1080/00423114.2023.2297799
[24] Lee T, Seo D, Lee J, et al. Real-time drift-driving control for an autonomous vehicle: learning from nonlinear model predictive control via a deep neural network. Electronics (Basel). 2022;11(17):2651. doi:10.3390/electronics11172651

[25] Ding N, Thompson M, Dallas J, et al. Drifting with unknown tires: learning vehicle models online with neural networks and model predictive control. In: 2024 IEEE Intelligent Vehicles Symposium (IV); 2-5 June 2024; 2024. p. 2545–2552. doi: 10.1109/IV55156.2024.10588474.
[26] Miller B. McLaren variable drift control: does it work? https://www.carmagazine.co.uk/car-news/tech/mclaren-variable-drift-control-how-does-it-work/.
[27] Duff M. Thank you for smoking: ford explains the focus RS's "Drift mode". https://www.caranddriver.com/news/a15357160/thank-you-for-smoking-ford-explains-the-focus-rss-drift-mode/.
[28] GmbH BM. The M drift analyser for BMW M3 and M4. https://www.bmw-m.com/en/topics/magazine-article-pool/bmw-m3-m4-m-drift-analyser.html.
[29] Sun Y, Velenis E, Krishnakumar A. Evaluation of an intuitive 4WD drift assist control concept in a driving simulator. Veh Syst Dyn. 2025. doi:10.1080/00423114.2025.2487186
[30] Eberhart M, Plöchl M, Unterreiner M, et al. Insights into stability and control of the powerslide motion with variable drive torque distribution – applied to a driver assistance system. Veh Syst Dyn. 2025:1–21. doi:10.1080/00423114.2025.2457433
[31] Jaumann F, Schuster T, Unterreiner M, et al. Powerslide control with deep reinforcement learning. In: G. Mastinu, F. Braghin, F. Cheli, M. Corno, and S. M. Savaresi, editors. 16th International Symposium on Advanced Vehicle Control. Cham: Springer Nature Switzerland; 2024. p. 862–868.
[32] Sun Y, Velenis E, Krishnakumar A. Steering noise cancelling for drift assist control. In: G. Mastinu, F. Braghin, F. Cheli, M. Corno, and S. M. Savaresi, editors. 16th International Symposium on Advanced Vehicle Control, Cham: Springer Nature Switzerland; 2024. p. 618–624.
[33] Joa E, Cha H, Hyun Y, et al. A new control approach for automated drifting in consideration of the driving characteristics of an expert human driver. Control Eng Pract. 2020;96:104293. doi:10.1016/j.conengprac.2019.104293
[34] Vignati M, Sabbioni E, Cheli F. A torque vectoring control for enhancing vehicle performance in drifting. Electronics (Basel). 2018;7(12):394. doi:10.3390/electronics7120394
[35] Park M, Kang Y. Experimental verification of a drift controller for autonomous vehicle tracking: a circular trajectory using LQR method. Int J Control Autom Syst. 2021;19(1):404–416. doi: 10.1007/s12555-019-0757-2
[36] Weng W, Hu C, Li Z, et al. An aggressive cornering framework for autonomous vehicles combining trajectory planning and drift control. In: 2024 IEEE Intelligent Vehicles Symposium (IV); 2-5 June 2024; 2024. p. 2749–2755.
[37] Kim M, Lee T, Kang Y. Experimental verification of the power slide driving technique for control strategy of autonomous race cars. Int J Prec Eng Manuf . 2020;21(3):377–386. doi:10.1007/s12541-019-00263-1
[38] Pereiras VF. Drift control with driver in the loop. MSc, School of Aerospace, Transport and Manufacturing, Cranfield University; 2022.
[39] Guo W, et al. Toward consumer acceptance of cooperative driving systems: a human-centered shared steering control approach within a hierarchical framework. IEEE Trans Consum Electron. 2024;70(1):635–645. doi:10.1109/TCE.2024.3357985
[40] Xing Y, Lv C, Mo X, et al. Toward safe and smart mobility: energy-aware deep learning for driving behavior analysis and prediction of connected vehicles. IEEE Trans Intell Transp Syst. 2021;22(7):4267–4280. doi: 10.1109/TITS.2021.3052786
[41] Aksjonov A, Nedoma P, Vodovozov V, et al. Detection and evaluation of driver distraction using machine learning and fuzzy logic. IEEE Trans Intell Transp Syst. 2019;20(6):2048–2059. doi:10.1109/TITS.2018.2857222
[42] Ersal T, Fuller HJA, Tsimhoni O, et al. Model-based analysis and classification of driver distraction under secondary tasks. IEEE Trans Intell Transp Syst. 2010;11:692–701. doi:10.1109/TITS.2010.2049741
[43] Vellenga K, Steinhauer HJ, Karlsson A, et al. Driver intention recognition: state-of-the-art review. IEEE Open J Intell Transp Syst. 2022;3:602–616. doi:10.1109/OJITS.2022.3197296

[44] Leonhardt V, Pech T, Wanielik G. Data fusion and assessment for maneuver prediction including driving situation and driver behavior. In: 2016 19th International Conference on Information Fusion (FUSION); 5-8 July 2016; 2016. p. 1702–1708.
[45] Liu J, Luo Y, Xiong H, et al. An integrated approach to probabilistic vehicle trajectory prediction via driver characteristic and intention estimation. In: 2019 IEEE Intelligent Transportation Systems Conference (ITSC), 27-30 Oct. 2019; 2019. p. 3526–3532. doi: 10.1109/ITSC.2019.8917039.
[46] Tran D, Sheng W, Liu L, et al. A hidden Markov model based driver intention prediction system. In 2015 IEEE International Conference on Cyber Technology in Automation, Control, and Intelligent Systems (CYBER); 2015. p. 115–120.
[47] Peng J, Guo Y, Fu R, et al. Multi-parameter prediction of drivers' lane-changing behaviour with neural network model. Appl Ergon. 2015;50:207–217. doi:10.1016/j.apergo.2015.03.017
[48] Il-Hwan Kim J-HB, Park J, Park S. Prediction of driver's intention of lane change by augmenting sensor information using machine learning techniques. Sensors. 2017;17(6:):1350. doi:10.3390/s17061350
[49] Xing Y, Lv C, Wang H, et al. An ensemble deep learning approach for driver lane change intention inference. Transp Res C, Emerg Technol. 2020;115:102615. doi:10.1016/j.trc.2020.102615
[50] Gite S, Agrawal H, Kotecha K. Early anticipation of driver's maneuver in semiautonomous vehicles using deep learning. Prog Artif Intell. 2019;8(3):293–305. doi:10.1007/s13748-019-00177-z
[51] Hao Z, Huang X, Wang K, et al. Attention -based GRU for driver intention recognition and vehicle trajectory prediction. In 2020 4th CAA International Conference on Vehicular Control and Intelligence (CVCI); 18-20 Dec. 2020; 2020. p. 86–91. doi: 10.1109/CVCI51460.2020.9338510.
[52] Benterki A, Boukhnifer M, Judalet V, et al. Artificial intelligence for vehicle behavior anticipation: hybrid approach based on maneuver classification and trajectory prediction. IEEE Access. 2020;8:56992–57002. doi:10.1109/ACCESS.2020.2982170
[53] Shangguan Q, Fu T, Wang J, et al. A proactive lane-changing risk prediction framework considering driving intention recognition and different lane-changing patterns. Accid Anal Prev. 2022;164:106500. doi:10.1016/j.aap.2021.106500
[54] Xie D-F, Fang Z-Z, Jia B, et al. A data-driven lane-changing model based on deep learning. Transp Res C, Emerg Technol. 2019;106:41–60. doi:10.1016/j.trc.2019.07.002
[55] Jain A, Koppula HS, Raghavan B, et al. Car that knows before you do: anticipating maneuvers via learning temporal driving models. In: Presented at the Proceedings of the 2015 IEEE International Conference on Computer Vision (ICCV); 2015. [Online]. https://doi.org/10.1109/ICCV.2015.364
[56] Chen Y, Cao H, Xiang Z, et al. Vehicle lane-change intention recognition based on BiLSTM attention model for the internet of vehicles. Proc Inst Mech Eng D: J Automob Eng. 2024;239(7):2551–2564. doi:10.1177/09544070241240225
[57] Díaz-Álvarez A, Clavijo M, Jiménez F, et al. Inferring the driver's lane change intention through LiDAR-based environment analysis using convolutional neural networks. Sensors. 2021;21(2):475. doi:10.3390/s21020475
[58] Leonhardt V, Wanielik G. Feature evaluation for lane change prediction based on driving situation and driver behavior. In: 2017 20th International Conference on Information Fusion (Fusion), 10-13 July 2017; 2017. p.1–7. doi: 10.23919/ICIF.2017.8009848
[59] Tang L, Wang H, Zhang W, et al. Driver lane change intention recognition of intelligent vehicle based on long short-term memory network. IEEE Access. 2020;8:136898–136905. doi:10.1109/ACCESS.2020.3011550
[60] Cui G, Huang H. Enhancing driver maneuver intention recognition: a framework integrating driver facial motion and driving scene understanding. In: 2024 IEEE 20th International Conference on Automation Science and Engineering (CASE); 28 Aug.-1 Sept. 2024; 2024. p. 3999–4004. doi: 10.1109/CASE59546.2024.10711400

[61] Doshi A, Trivedi MM. Investigating the relationships between gaze patterns, dynamic vehicle surround analysis, and driver intentions. In: 2009 IEEE Intelligent Vehicles Symposium; 2009. p. 887–892.
[62] Li M, Cao H, Song X, et al. Shared control driver assistance system based on driving intention and situation assessment. IEEE Trans Ind Inf. 2018;14(11):4982–4994. doi:10.1109/TII.2018.2865105
[63] Kouchak SM, Gaffar A. Detecting driver behavior using stacked long short term memory network with attention layer. IEEE Trans Intell Transp Syst. 2021;22(6):3420–3429. doi:10.1109/TITS.2020.2986697
[64] Mänttäri J, Folkesson J, Ward E. Learning to predict lane changes in highway scenarios using dynamic filters on a generic traffic representation. In: 2018 IEEE Intelligent Vehicles Symposium (IV); 26-30 June 2018; 2018. p. 1385–1392. doi: 10.1109/IVS.2018.8500426
[65] Li J, Mei X, Prokhorov D, et al. Deep neural network for structural prediction and lane detection in traffic scene. IEEE Trans Neural Networks Learn Syst. 2017;28(3):690–703. doi:10.1109/TNNLS.2016.2522428
[66] Li MG, Jiang B, Che Z, et al. DBUS: human driving behavior understanding system. In: 2019 IEEE/CVF International Conference on Computer Vision Workshop (ICCVW); 27-28 Oct. 2019; 2019. p. 2436–2444. doi: 10.1109/ICCVW.2019.00298
[67] Behera A, Wharton Z, Keidel A, et al. Deep CNN, body pose, and body-object interaction features for drivers' activity monitoring. IEEE Trans Intell Transp Syst. 2022;23(3):2874–2881. doi:10.1109/TITS.2020.3027240
[68] Tan M, et al. Bidirectional posture-appearance interaction network for driver behavior recognition. IEEE Trans Intell Transp Syst. 2022;23(8):13242–13254. doi:10.1109/TITS.2021.3123127
[69] Li P, et al. Driver distraction detection using octave-like convolutional neural network. IEEE Trans Intell Transp Syst. 2022;23(7):8823–8833. doi:10.1109/TITS.2021.3086411
[70] Simulation K. Assetto Corsa. https://assettocorsa.gg/assetto-corsa/.
[71] Academy NM. Sim Racing Isn't Gaming, It's For Motorsport Pros! https://motorsport.nda.ac.uk/news/sim-racing-faster-driver/.
[72] Hardy E. Everything about Max Verstappen's sim racing career and his Le Mans ambitions. https://www.motorsport.com/lemans/news/all-to-know-about-max-verstappens-sim-racing-career-amid-le-mans-24-hours-ambition/10613885/.
[73] KLGreene. (ACTI) Assetto Corsa Telemetry Interface 1.1.2. https://www.overtake.gg/downloads/acti-assetto-corsa-telemetry-interface.3948/#:~:text=(ACTI)%20Assetto%20Corsa%20Telemetry%20Interface.
[74] MoTec. MoTeC i2 Data Analysis Software. https://www.motec.com.au/products/I2?catId=4.
[75] Graves A, Schmidhuber J. Framewise phoneme classification with bidirectional LSTM and other neural network architectures. Neural Netw. 2005;18(5):602–610. doi:10.1016/j.neunet.2005.06.042
[76] Chung J, Gulcehre C, Cho K, et al. Empirical evaluation of gated recurrent neural networks on sequence modeling; 2014.
[77] Hochreiter S, Schmidhuber J. Long short-term memory. Neural Comput. 1997;9:1735–1780. doi:10.1162/neco.1997.9.8.1735
[78] Karaman Y, Akdeniz F, Kir Savaş B, et al. A comparative analysis of SVM, LSTM and CNN-RNN models for the BBC news classification; 2023.p. 473–483.
[79] Kingma DP, Ba J. Adam: a method for stochastic optimization. CoRR, vol. abs/1412.6980; 2014.
[80] Bishop CM. Pattern recognition and machine learning (information science and statistics). New York: Springer-Verlag; 2006.
[81] Ting KM. Confusion matrix. In: C Sammut, GI Webb, editors. Encyclopedia of machine learning. Boston, MA: Springer US; 2010. p. 209–209.



https://dspace.org/

Toward intuitive drift assist control: driver drift intention recognition using a data-based approach

Sun, Yiwen; Velenis, Efstathios; Krishnakumar, Ajinkya

2025-12-31
Taylor & Francis
https://doi.org/10.1080/00423114.2025.2520492
Sun Y, Velenis E, Krishnakumar A. (2025) Toward intuitive drift assist control: driver drift intention recognition using a data-based approach. Vehicle System Dynamics, Available online 28 June 2025

Downloaded from a DSpace repository. https://dspace.org/